Chemistry and Physics of Lipids 221 (2019) 39–45

Contents lists available at ScienceDirect

Chemistry and Physics of Lipids

journal homepage: www.elsevier.com/locate/chemphyslip

Solvent accessibility in interdigitated and micellar phases formed by DPPC/Lyso-PPC mixtures: D_2O-ESEEM of chain labeled lipids

Erika Aloi, Rosa Bartucci*

Department of Physics, Molecular Biophysics Laboratory, University of Calabria, 87036 Rende, CS, Italy

ARTICLE INFO

Keywords:
DPPC
Lyso-PPC
Interdigitated lamellae
Micelles
D2O-ESEEM
Spin-label
Water penetration profile

ABSTRACT

Electron spin echo envelope modulation (ESEEM) spectroscopy was used to investigate binary mixtures of single-chain micelle-forming lipids and diacyl bilayer-forming lipids dispersed in D_2O at 77 K. Mixtures of dipalmitoylphosphatidylcholine (DPPC) and lyso-palmitoylphosphatidylcholine (Lyso-PPC) over the entire composition range (0–100 mol%) and phosphatidylcholine spin-labeled at selected carbon atom position along the *sn*-2 chain (*n*-PCSL) were considered. On increasing the content of the lysolipids incorporated in DPPC, the lipid bilayers are first transformed in interdigitated lamellae and then converted in micelles of Lyso-PPC. In the interdigitated phase, the profile of translamellae water accessibility is rather uniform as all the hydrocarbon segments are equally exposed to the solvent. In Lyso-PPC micelle, water penetrates at any depth of the hydrocarbon region with a tendency to increase toward the chain termini. The extent of water penetration is higher in the interdigitated DPPC/Lyso-PPC dispersions than in Lyso-PPC micelles. The profiles of water permeation revealed directly by D_2O-ESEEM are also confirmed by more indirect evaluation of the polarity profiles based on the ^{14}N-hyperfine splitting in the conventional electron paramagnetic resonance spectra of *n*-PCSL in frozen DPPC/Lyso-PPC mixtures at 77 K. The ESEEM data reveal that H-bonding formation between the –NO group of the spin-label and the D_2O molecules is favored in the intergitated phase with respect to the micellar phase and, in any lipid dispersion, the fraction of nitroxides that are singly H-bonded to deuterons is higher than the fraction that are doubly H-bonded. The overall results highlight the differences in the accessibility and properties of the solvent in the hydrocarbon region of lipid bilayers, interdigitated bilayers and micelles.

1. Introduction

The penetration of the solvent in specific regions within biosystems, such as lipid assemblies and proteins, is an important biophysical aspect as it impacts on the permeability and transport properties of biomembranes, and on the stability and function of membrane proteins. Specifically, the water accessibility in the hydrocarbon region of phospholipid aggregates and the resulting hydrophobic barrier is an energetic determinant for the interaction of lipids with peptides and proteins and of lipid nanostructures with poorly water-soluble drugs.

For its sensitivity to environmental polarity, continuous wave electron paramagnetic resonance (cw-EPR) spectroscopy in combination with the use of chain-labeled lipids has proved to be an efficient tool to delineate the transmembrane polarity profiles via the dependence on chain label position of the three EPR polarity-sensitive spectral parameters, i.e., the isotropic ^{14}N-hyperfine coupling constant, A_0, the *z*-component of the hyperfine tensor, A_{zz}, and the *x* component of the *g*-value tensor, g_{xx}, at X-band and high field/high frequency (for a review, see Marsh, 2010).

Direct determination of solvent (D_2O) penetration at a given depth in the hydrophobic region of lipid aggregates is possible by a pulse EPR technique, namely ^2H-electron spin echo envelope modulation (ESEEM). It involves the detection of the weak hyperfine interaction of the electron spin of a nitroxide label moiety with the nearby deuterium nuclear spin within a distance of about 0.5 nm. This interaction modulates the amplitude of the spin-echo decay at the nuclear hyperfine frequency (Dikanov and Tsvetkov, 1992; Schweiger and Jeschke, 2001). In the pioneering studies by Kevan and coworkers, the exposure to D_2O of different regions of spin-labeled frozen detergent micelles and vesicles has been detected by analyzing the modulation depth of the time domain decay of two-pulse ^2H-ESEEM (Szajdzinska-Pietek et al., 1984; Hiff and Kevan, 1989; Bratt et al., 1992). Later on, two- and three-pulse Fourier-Transform ^2H-ESEEM in the frequency domain has been used to map out the transmembrane polarity profile in model and natural membranes (Kurshev and Kevan, 1995; Bartucci et al., 2003a; Noethig-Laslo et al., 2004; Erilov et al., 2005; Bartucci et al., 2014;

* Corresponding author.
E-mail address: rosa.bartucci@fis.unical.it (R. Bartucci).

https://doi.org/10.1016/j.chemphyslip.2019.03.005
Received 23 January 2019; Received in revised form 27 February 2019; Accepted 11 March 2019
Available online 12 March 2019
0009-3084/

Oranges et al., 2018). Other biophysical applications of spin-label D_2O-ESEEM comprise the determination of the water permeation to specific regions of proteins (Volkov et al., 2009; Cieslak et al., 2010; Urban and Steinhoff, 2013), the localization of specific regions of membrane-active peptides (Carmieli et al., 2006; Salnikov et al., 2006) and proteins (Cieslak et al., 2010) within model membranes, and the capture of fatty acids by peptides and proteins (De Simone et al., 2007; Afanasyeva et al., 2019).

It is important to extend the D_2O-ESEEM studies to supramolecular aggregates formed by self-assembling of lipids of different species. Among others, molecular assemblies of interest are those formed by binary mixtures of bilayer-forming lipids, such as diacyl phosphatidylcholines, (PCs), and micelle-forming lipids, such as single-chain Lyso-phosphatidylcholines, (Lyso-PCs). PC-lipids are abundant in the cell membrane of eukaryotes and bacteria (van Meer et al., 2008). In particular, dipalmitoylphosphatidylcholine (DPPC) is a bilayer-forming lipid widely used for the preparation and biophysical characterization of cell membrane model systems, and DPPC bilayers represent an appropriate matrix in which other types of lipids can be incorporated (Lasic, 1993). Lyso-PCs are found in small amounts in mammalian cell membranes and in various membranes of subcellular organelles where they play a key role in cellular, physiological and pathological processes (Fuller and Rand, 2001; Ohata et al., 2001; Luquain et al., 2003). Synthetic Lyso-PCs are wedge shaped single-chain micelle-forming lipids (Arvidson et al., 1985) that, at low content, are essential components of PC-based thermosensitive liposomes used in drug delivery (Anyarambhatla and Needham, 1999; Needham et al., 2000).

Literature data report that Lyso-PC lipids show affinity for bilayers of PCs (van Echteld et al., 1980). However, when inserted in a host lipid model membrane, Lyso-PCs affect as a function of their concentration the order and the structure of the acyl chains (McIntosh et al., 1995; Lee and Chan, 1977; Bhamidipati and Hamilton, 1995; Lu et al., 1997, 2001; Mishima et al., 2004; Pantusa et al., 2008), the mechanical properties (Zhelev, 1988), and the permeability of lipid vesicles (Lee and Chan, 1977; van Echteld et al., 1981). It has been evidenced by using x-ray diffraction that the incorporation of 30 mol% (Lu et al., 2001) or 50 mol% (McIntosh et al., 1995) of Lyso-palmitoylphosphatidylcholine (Lyso-PPC) in bilayers of DPPC induces the formation of an interdigitated gel phase. The thermotropic phase behavior of fully hydrated DPPC/Lyso-PPC binary mixtures studied between 10 and 50 °C by spin-label cw-EPR and spectrophotometry showed a rich polymorphism characterized by the induction of a lamellar gel phase with interdigitated chains at intermediate content of Lyso-PPC and the conversion to micellar aggregates at high content of Lyso-PPC at any temperature (Pantusa et al., 2008).

In this work we investigate the lyotropic phase behavior of fully hydrated binary mixtures in D_2O of diacyl- and Lyso-lipids with identical polar head and acyl chain length, namely DPPC and Lyso-PPC over the entire composition range (0–100 mol% of Lyso-PPC) at 77 K. This is done by using three-pulse D_2O-ESEEM and phosphatidylcholines that are spin-labeled at selected carbon atom positions C-*n* along the *sn*-2 chain (*n*-PCSL, n = 5, 7, 8, 9, 10, 11, 12, 14 and 16). Emphasis is given to establish the profile of solvent penetration throughout the lipid chain in the interdigitated lamellar phase formed at intermediate content of Lyso-PPC incorporated in DPPC and in Lyso-PPC micelles. The solvent properties in the nearest hydration shell around the nitroxide spin-label group are also investigated.

2. Materials and methods

2.1. Materials

The synthetic lipids 1,2-dipalmitoyl-sn-glycero-3-phosphocholine (DPPC) and 1-palmitoyl-2-lyso-sn-glycero-3-phosphocholine (Lyso-PPC) and deuterium oxide (D_2O) (99.9 atom% ^2H) were obtained from Sigma/Aldrich (St. Louis, MO). The spin-labeled lipids 1-palmitoyl-2-(n-(4,4-dimethyl-oxazolidine-*N*-oxyl) stearoyl)-*sn*-glycero-3-phosphocholine (*n*-PCSL with n = 5, 7, 8, 9, 10, 11, 12, 14 and 16) were either from Avanti Polar Lipids (Birmingham, AL) or synthesized as described elsewhere (Marsh and Watts, 1982). All materials were used as purchased without further purification.

2.2. Sample preparation

Hand shaken lipid dispersions were prepared by dissolving in chloroform the required amounts of DPPC and Lyso-PPC together with 0.5 mol% of the spin-labeled lipid *n*-PCSL. The solvent was first evaporated in a nitrogen gas stream and then under vacuum overnight. The dried lipid samples were fully hydrated with D_2O (final lipid concentration 50 mM), by heating and vortexing at 50 °C. The hydrated lipid dispersions were concentrated at room temperature by centrifugation at 3000 rpm for 20 min in a bench-top centrifuge, the excess of water removed (the samples float in D_2O) and the pellets transferred to standard (O.D. 4 mm) quartz EPR tubes for FT- and CW-EPR measurements.

2.3. EPR measurements

Pulsed EPR data were collected at 77 K on an ELEXSYS E580 9-GHz Fourier Transform FT-EPR spectrometer (Bruker, Germany) equipped with a MD5 dielectric resonator and a CF 935 P cryostat (Oxford Instruments, UK).

To obtain ESEEM spectra, three-pulse, stimulated echo ($\pi/2$-τ-$\pi/2$-T-$\pi/2$-τ-echo) decays were recorded by using microwave pulse widths of 12 ns, with the microwave power adjusted to give $\pi/2$-pulses. The time delay, T, between the second and the third pulses was incremented from 20 ns by 700 steps of 12 ns, whilst the inter-pulse separation, τ, between the first and second pulses was set equal to 168 ns to maximize the deuterium and proton modulations simultaneously. The magnetic field was set to the maximum of the EPR absorption. A four-step phase-cycling program was used to eliminate unwanted echoes. For obtaining standardized ESEEM intensities, the time-dependent echo amplitudes were processed according to a protocol previously developed (Erilov et al., 2005): 1) the average experimental echo decay was fitted with a biexponential function; 2) the data were divided by the fitted average decay function, so that only oscillations about unity remained; 3) the unit level was subtracted from the signal; 4) three levels of zero filling were added at the end of the ESEEM data to increase the total number of points to 4 K; 5) numerical Fourier transformation was performed to obtain an absolute-value ESEEM spectrum. The dwell time (ΔT = 12 ns) was specifically included between points thus providing machine-independent spectral density with the dimensions of time (Bartucci et al., 2009).

For 3p-ESEEM experiments, samples were rapidly frozen in liquid nitrogen and then quickly accommodated into the pre-cooled cavity at 77 K.

Conventional CW-EPR spectra were acquired at 77 K on a Bruker ESP-300 spectrometer operating at 9 GHz with 100-kHz field modulation and equipped with a Bruker ER 4201 TE_{102} rectangular cavity. For CW-EPR measurements, the samples in the quartz tubes were first rapidly frozen in liquid nitrogen and then introduced into a finger dewar containing liquid nitrogen.

Spin-label EPR measurements were repeated two or three times on newly prepared samples. Representative spectra are shown in the figures, whereas the data points are averages ± standard deviations.

3. Results and discussion

3.1. D_2O-ESEEM of 5- and 16-PCSL: lyotropic phase behavior of DPPC/Lyso-PPC frozen dispersions

Three-pulse ($\pi/2$-τ-$\pi/2$-T-$\pi/2$-τ-echo) spin-label D_2O-ESEEM

measurements have been carried out to detect the solvent accessibility in the hydrocarbon region of the different phases formed by adding increasing amounts of Lyso-PPC in DPPC bilayers that are hydrated in D_2O. To do this, as first step, the decays of the maximum amplitude of the stimulated echo vs. the interpulse spacing, T, at fixed $\tau = 168$ ns have been collected. Fig. S1 gives the electron spin echo decays at 77 K for 5- and 16-PCSL in selected DPPC/Lyso-PPC/D_2O dispersions. The decay curves show two modulations: superimposed to a slow modulation with a period of about 0.4 μs, there is a rapid oscillation with a period of about 0.07 μs. The slow modulation is due to dipolar interactions of the spin-label with the ^{2}H-nuclear spin of the D_2O molecules, whereas the rapid modulation arises from interactions of the electron spin with nearby protons. The modulation by D_2O is of interest because it comes specifically from the solvent. From Fig. S1 it is clearly evident that for 16-PCSL the slow ^{2}H-modulation is absent in the DPPC sample and starts to appear in the mixture with the lowest Lyso-PPC content. Visualization and quantitation of the ^{2}H-modulation is better achieved after Fourier transformation, which yields the spectrum in the nuclear frequency domain (see Materials and Methods).

Absolute-value frequency ESEEM spectra for *5*- and 16-PCSL in DPPC dispersions in the presence of different concentration of Lyso-PPC are shown in Fig. 1.

The spectra show lines that are centered around the deuterium ^{2}H-Larmor frequency at ca. 2.5 MHz and around the proton ^{1}H-Larmor frequency at ca. 15 MHz. The latter originates from matrix protons, whereas the former is specifically due to the solvent molecules. The deuterium ^{2}H-ESEEM signals consist of a sharp doublet superimposed to a broad component. The sharp component arises from free, not H-bonded D_2O molecules to the spin-label nitroxide -NO group, whereas the broad component is from H-bonded D_2O molecules to the nitroxide moiety (Erilov et al., 2005).

The effects of Lyso-PPC content on the spectral density of the above ESEEM spectra can be quantified by measuring the total amplitude of the deuterium ESEEM signal, I(^{2}H). The amplitude is proportional to the number of D_2O molecules neighboring the spin label and, therefore, gives a direct measure of the extent of water (D_2O) penetration at the labeling site (Erilov et al., 2005). I(^{2}H) for 5- and 16-PCSL as a function of Lyso-PPC content in frozen DPPC/Lyso-PPC mixtures is reported in Fig. 2.

As it can be seen, in DPPC bilayers (0 mol% Lyso-PPC), for 5-PCSL, which probes the first methyl segments of the hydrocarbon region, there is an evident ^{2}H-peak, whereas for 16-PCSL, which probes the inner hydrocarbon region at the bilayer midplane, the deuterium signal is almost completely absent. This is an expected result for the two extreme positions of chain labeling in frozen DPPC bilayers. Indeed, through cw- and pulsed EPR of *n*-PCSL in DPPC bilayers, a sigmoidal transmembrane profile of polarity and solvent penetration is generally recorded in which the region close to the polar/apolar interface is of high polarity and accessible to the solvent whereas the innermost hydrocarbon region has reduced polarity and inaccessible to the solvent

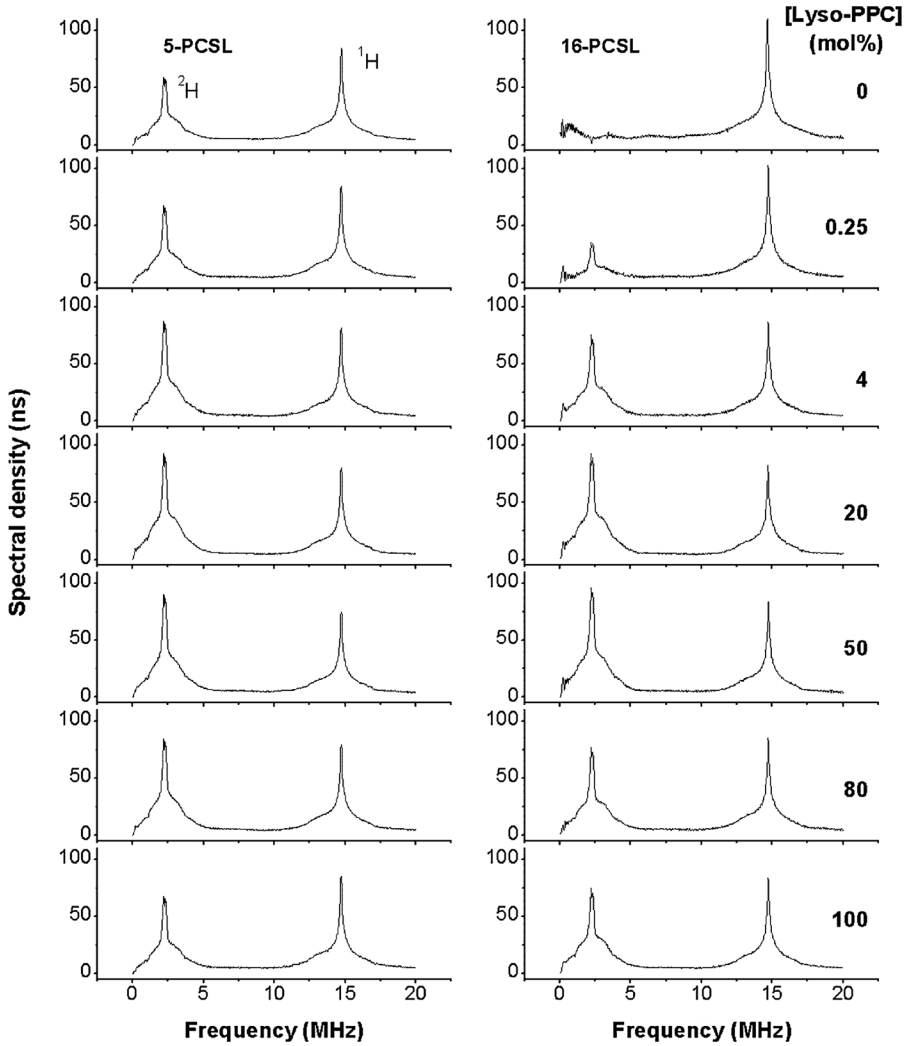

Fig. 1. Fourier Transform ESEEM spectra at 77 K for 5-PCSL (left panel) and 16-PCSL (right panel) in mixtures of DPPC and selected concentration of Lyso-PPC hydrated in D_2O.

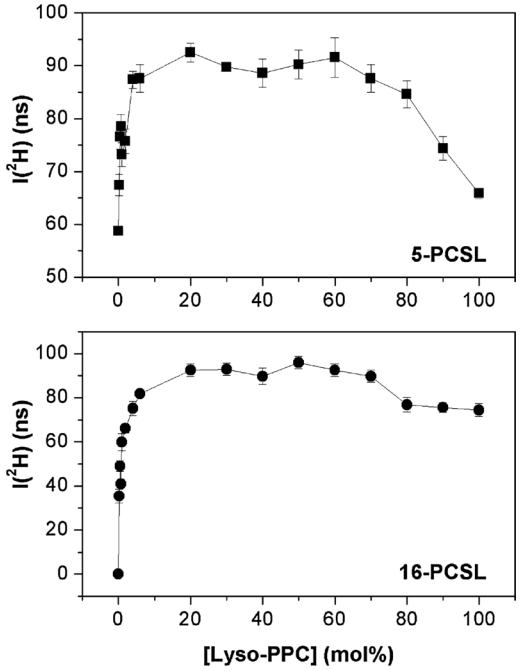

Fig. 2. Dependence on Lyso-PPC concentration of the deuterium spectral amplitudes, I(^{2}H), at 77 K for 5-PCSL (squares) and 16-PCSL (circles) in DPPC/Lyso-PPC mixtures hydrated in D_2O.

(Marsh, 2001; Bartucci et al., 2003a; Erilov et al., 2005). This corresponds to a decrease in the local concentration of intramembranous water (D_2O) on going from the first segments towards the center of lipid bilayers.

In the presence of Lyso-PPC, 5-PCSL displays in any sample an evident ^{2}H-signal whose intensity increases first rapidly with the addition of low content up to ca. 5 mol% of Lyso-PPC and then more slowly, reaching a plateau value at ca. 20 mol%. I(^{2}H) maintains this high value up to ca. 60–70 mol% and finally it decreases reaching in micelles of pure Lyso-PPC a value slightly higher than that recorded in DPPC bilayers (see left panel of Fig. 1 and upper panel of Fig. 2).

It is interesting to note that for 16-PCSL the deuterium peak shows up already at the lowest Lyso-lipid concentration. I(^{2}H) for 16-PCSL chain-end positional isomer increases steeply and markedly, reaching at 20 mol% a high value comparable to that of 5-PCSL and maintaining it up to ca. 60–70 mol%. Then the signal intensity slightly decreases and becomes independent on Lyso-PPC content for concentration ≥ 80 mol % (see right panel in Fig. 1 and lower panel of Fig. 2).

The ESEEM results in the Figs. 1 and 2 obtained at 77 K in rapidly-frozen samples show the variation in the accessibility of the solvent around the C-5 and C-16 positions in the hydrocarbon zone of the interdigitated lamellae and micelles that are progressively formed upon adding increasing amount of the Lyso-lipids in DPPC bilayers. The most likely interpretation of the data is that lamellae with interdigitated chains exist for Lyso-PPC content between 20 and 70 mol% and then micelles rich of Lyso-lipids and Lyso-PPC micelles are formed.

Relative to DPPC bilayers with noninterdigitated chains, in the lamellar organization with interdigitated chains i) the I(^{2}H)-values for 5-PCSL are higher because of the expansion in the area for polar head that accompanies the formation of the interdigitated phase induced by the insertion of the Lyso-lipids in DPPC; ii) 16-PCSL becomes accessible to the solvent because of the transfer of apolar groups towards the polar/apolar interface; iii) the two positional isomers 5- and 16-PCSL have almost the same D_2O intensity signal, i.e., they are equally exposed to the solvent, because they probe the same hydrocarbon region at the polar zone.

The ESEEM data in Lyso-PPC micelles (Figs. 1 and 2 for [Lyso-PPC] ≥ 80 mol%) show that solvent permeates the hydrocarbon region not only at the beginning of the chain (probed by 5-PCSL) to an extent comparable to that in the polar region of DPPC bilayers, but also at the chain termini (probed by 16-PCSL) that is inaccessible to water in DPPC bilayers.

3.2. Interdigitated lamellar phase of DPPC/Lyso-PPC: water accessibility and polarity profiles

To delineate the profile of water accessibility across the hydrocarbon region in the interdigitated and micellar phases formed by frozen DPPC/Lyso-PPC/D_2O mixtures, ESEEM measurements have also been carried out by using chain labeled phosphatidylcholines at additional positions besides 5- and 16-PCSL. For the water penetration profile in the interdigitated phase, we report the results relative to the sample composed of DPPC and 50 mol% Lyso-PPC. Analogous results have been obtained by measuring selected positional isomers in samples with lower (i.e., 40 mol%) and higher (i.e., 60 mol%) content of the Lyso-lipid.

The dependence of the ^{2}H-ESEEM intensity on chain segment position of *n*-PCSL in frozen interdigitated dispersions DPPC/Lyso-PPC 1:1 mol/mol in Fig. 3 indicates that all the chain segments are exposed to the solvent to a similar extent.

The I(^{2}H)-values for positions of labeling close to the lipid polar head groups (n = 5–9) are comparable to those close to the chain termini (n = 14–16) and slightly lower than those between n = 10 and n = 12. All these values are higher than those recorded in the upper hydrocarbon region of noninterdigitated DPPC bilayers (n = 4–11) and rather similar to those of DPPC/cholesterol 1:1 mol/mol bilayers with noninterdigitated chains (n = 4–7) characterized by significant water accessibility (Erilov et al., 2005). When compared to DPPC bilayers, both DPPC/Lyso-PPC and DPPC/Cholesterol samples are more exposed to solvent at the polar/apolar interface as the wedge shaped Lyso-lipids and the intervening cholesterol molecules space apart the polar heads allowing higher hydration at the interfacial region of the dispersions. The I(^{2}H)-values for any *n*-PCSL isomer in the interdigitated phase of DPPC/Lyso-PPC are typical of hydrocarbon environments and are much smaller than those of *n*-SASL in the hydrophobic binding pockets of human serum albumin (De Simone et al., 2007) and in the calyx of β-lactoglobulin (Guzzi et al., 2012).

Information on the variation of polarity across the hydrocarbon region of interdigitated DPPC/Lyso-PPC have been obtained by cw-EPR spectra of chain-labeled lipids in rapidly frozen samples at 77 K. The spectra of all positional isomers are powder patterns of immobilized spin-labels on the conventional EPR time-scale (see Fig. S2). The outermost peak separation, $2A_{zz}$, of the cw-EPR spectra whose lineshapes

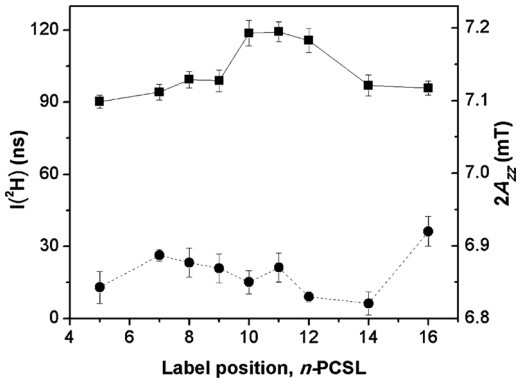

Fig. 3. Dependence on spin-label position, *n*, of the deuterium spectral amplitude, I(^{2}H) (solid line and left-hand scale), and of the outermost peak separation, $2A_{zz}$ (dashed line and right-hand scale), for spin-labeled phosphatidylcholine *n*-PCSL in interdigitated lamellar dispersions of DPPC and 50 mol% Lyso-PPC hydrated in D_2O. T = 77 K.

are devoid of motional averaging is sensitive to environmental polarity and proticity (Marsh, 2010). The positional dependence of $2A_{zz}$ in Fig. 3 delineates an almost uniform profile of elevated polarity with $2A_{zz}$-values (ca. 6.8–6.9 m T) typical of the polar hydrophobic environment of a variety of lipid lamellae including bilayers of PCs and cholesterol (Subczynski et al., 1994; Bartucci et al., 2003a; Kurad et al., 2003).

It is worthy to note that the water penetration and the polarity profiles established respectively by ^{2}H-ESEEM and cw-EPR spectroscopy of chain labeled lipids *n*-PCSL in frozen interdigitated dispersions of DPPC + 50 mol% Lyso-PPC, reported in Fig. 3, mirror those previously reported in the interdigitated phase spontaneously adopted by ether-linked dialkyl-lipids of dihexadecyl phosphatidylcholine (Oranges et al., 2018).

On the whole, the solvent permeation and polarity profiles recorded by pulse and conventional spin-label EPR suggest that the molecular packing of lipid lamellae with interdigitated chains, both in single specie lipids (such as DHPC) and in mixtures (such as DPPC/Lyso-PPC) forms a hydrophobic cavity where all the methylene segments are accessible to solvent and of elevated polarity. The loss of the bilayer midplane in the interdigitated phase abolishes the sigmoidal polarity and the water accessibility profiles, which are typical of bilayers with noninterdigitated chains, just as it suppresses the limited chain-flexibility profile of increasing disorder and mobility on moving from the polar/apolar interface toward the terminal methyl end, which is detected in bilayers in the gel state by using cw-ESR of chain-labeled lipids (Boggs et al., 1989; Bartucci et al., 1993).

3.3. Micellar phase of Lyso-PPC: water accessibility and polarity profiles

D_2O-ESEEM and cw-EPR spectra of *n*-PCSL have been recorded at 77 K in micelle dispersions formed by Lyso-PPC at full hydration. The positional dependences of ^{2}H-ESEEM intensity, I(^{2}H), and of the outermost peak separation, $2A_{zz}$, in Fig. 4 show that I(^{2}H) decreases slightly at the first carbon atom positions and then moderately increases from the $n = 12$ position onwards. Similarly, $2A_{zz}$ decreases slowly up to $n = 12$ and then increases at the chain termini.

The I(^{2}H) and $2A_{zz}$-values of *n*-PCSL in frozen Lyso-PPC micelles are lower than those determined in frozen interdigitated DPPC/Lyso-PPC phase and are in the same range of variability of those previously reported for the upper apolar region in frozen DPPC bilayers (Subczynski et al., 1994; Bartucci et al., 2003a; Erilov et al., 2005). The D_2O-ESEEM and cw-EPR results for *n*-PCSL in Lyso-PPC micelles at 77 K are in close agreement with the polarity profile established with cw-EPR by measuring the isotropic hyperfine splitting, A_0, of stearic acids spin labeled at selected carbon atom position along the chain (*n*-SASL) in Lyso-PPC micelles at 50 °C (Bartucci et al., 2003b). By comparing the results in micelles obtained at low temperature in the present study with those at high temperature in (Bartucci et al., 2003b), it is evident that the minimum-value in the profiles is shifted toward slightly lower *n* ($n = 10$) in the fluid state. This is a feature that differentiates frozen from fluid lipid assemblies. It is worthy to note that it has also been found that the midpoint of the sigmoidal water accessibility and polarity profiles in chain-labeled DPPC membranes occurs at higher *n* in the frozen state (Erilov et al., 2005) than in the fluid state (Marsh, 2001). Similar to our results, two-pulse D_2O-ESEEM data in the time domain for 5-, 7- and 10-doxyl stearic acid in small micelles indicated water penetration at any depth in their hydrophobic zone (Szajdzinska-Pietek et al., 1984).

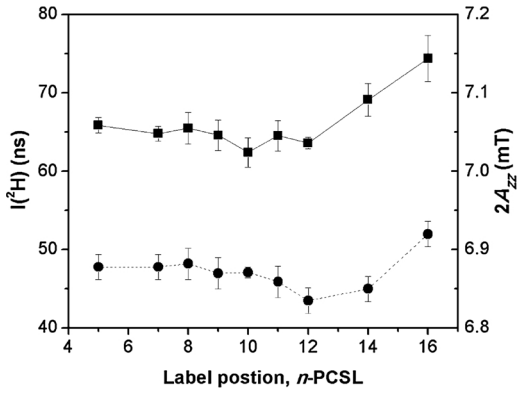

Fig. 4. Dependence on spin-label position, *n*, of the deuterium spectral amplitude, I(^{2}H) (solid line and left-hand scale), and of the outermost peak separation, $2A_{zz}$ (dashed line and right-hand scale), for spin-labeled phosphatidylcholine *n*-PCSL in Lyso-PPC micelles hydrated in D_2O. T = 77 K.

The profiles in Fig. 4 in which the terminal methyl ends are exposed to the solvent likely reflect the conformational disorder of the chains in small micelles of single chain lipids.

3.4. Solvent properties: H-bonding formation

The analysis of the D_2O-signal of the frequency domain ESEEM spectra of *n*-PCSL in DPPC/Lyso-PPC mixtures gives information on H-bond formation of the solvent with the nitroxide moiety -NO of the spin-label within 0.5 nm (Erilov et al., 2005).

From the intensity of the broad component, which is due to nitroxides H-bonded to the solvent, it is possible to evaluate the fraction of nitroxides that are singly, f_{1w}, and doubly bonded, f_{2w}, to D_2O. As previously shown by application of the mass-action law, the product of the equilibrium constant, *K*, for hydrogen bonding and the effective concentration of free water, [W], is related to the normalized intensity, I_{broad}, of the broad D_2O-ESEEM component by (Erilov et al., 2005):

$$K[W] = \frac{I_{broad}/I_o}{2 - I_{broad}/I_o}$$

where I_0 (≈115 ns) is the normalized ^{2}H-ESEEM intensity for a nitroxide with a single hydrogen-bonded D_2O molecule that is predicted by DFT calculations.

Correspondingly, the fraction of spin-labeled –NO groups that is H-bonded by a single water molecule is given by:

$$f_{1w} = \frac{2}{1/K[W] + 2 + K[W]}$$

The fraction of spin-labeled –NO groups that is H-bonded by two water molecules is then given by:

$$f_{2w} = \frac{1}{2}\left(\frac{I_{broad}}{I_0} - f_{1w}\right)$$

The results of *n*-PCSL in interdigitated DPPC/Lyso-PPC lamellae and in Lyso-PPC micelles are reported in Table 1.

From the data it can be observed that i) water penetration is higher in interdigitated lamellae than in micellar dispersions and ii) $f_{1w} > f_{2w}$ in any type of aggregate.

In DPPC/50 mol% Lyso-PPC interdigitated layers, the fraction of nitroxides that are H-bonded by a single water molecule varies from 0.32 to 0.38, and those that are H-bonded by two water molecules varies from 0.04 to 0.07; in Lyso-PPC micelles f_{1w} and f_{2w} vary between 0.19 and 0.23 and from 0.01 to 0.02, respectively. For comparison, the maximum values that are obtained in DPPC bilayers at the position $n = 5$ are 0.18 and ca. 0.01 for the fractions H-bonded to one and two waters, respectively, whereas for DPPC + 50 mol% cholesterol they were 0.36 and 0.06 (Erilov et al., 2005).

These results highlight the differences in the properties of the solvent along the lipid chain that result from the different modes of chain packing in the various lipid assemblies, i.e., normal and interdigitated lamellar phases and micelles.

Table 1
Fractions of *n*-PCSL hydrogen bonded by one (f_{1w}) and two (f_{2w}) water molecules from ^{2}H-ESEEM spectra of DPPC/Lyso-PPC dispersions in D_2O. The errors for f_{1w} and f_{2w} are within 5% and 10%, respectively.

n-PCSL	f_{1w}	f_{2w}
DPPC		
5	0.18	0.009
DPPC/Lyso-PPC interdigitated lamellae		
5	0.32	0.040
7	0.32	0.041
8	0.35	0.053
9	0.34	0.048
10	0.38	0.066
11	0.38	0.074
12	0.37	0.059
14	0.33	0.042
16	0.32	0.040
Lyso-PPC micelles		
5	0.19	0.011
7	0.21	0.014
8	0.21	0.014
9	0.21	0.014
10	0.20	0.013
11	0.21	0.014
12	0.21	0.015
14	0.22	0.016
16	0.23	0.017

4. Conclusions

In this work, three pulse ESEEM by D_2O has been employed to study mixtures of bilayer-forming DPPC lipids and micelle-forming Lyso-PPC lipids rapidly frozen at 77 K. The overall results indicate that D_2O-ESEEM combined with the use of chain-labeled lipids is a valuable tool to investigate the lyotropic phase behavior of the fully hydrated lipid mixtures and to characterize the profile of water penetration across the hydrocarbon region of the different formed mesophases. These comprise interdigitated lamellae over a wide composition range (20–70 mol % Lyso-PPC) and micelles ([Lyso-PPC] $\geq$ 80 mol%).

Relative to conventional, noninterdigitated DPPC bilayers, the extent of water permeation is increased in the frozen interdigitated phase of DPPC/Lyso-PPC mixtures at any chain position and almost uniform profiles of solvent accessibility and polarity across the hydrocarbon zone are recorded. Chain interdigitation suppresses the sigmoidal trans-hydrocarbon water penetration and polarity profiles usually reported in lipid bilayers and the I(^{2}H)- and $2A_{zz}$-values of *n*-PCSL in the interdigitated samples correspond to those obtained in other hydrocarbon lipid environments (DPPC/cholesterol at equimolar ratio, DHPC interdigitated lamellae) with packing properties similar to interdigitated DPPC/Lyso-PPC samples.

Frozen Lyso-PPC micelles are found to be less hydrated than interdigitated DPPC/Lyso-PPC mixtures and D_2O can access at any chain segments with a tendency to increase at the chain termini. The extent of water accessibility through the chains of Lyso-PPC micelles is comparable to that reported for the polar region of DPPC bilayers.

From a biophysical standpoint, the molecular properties evidenced in this work are relevant for lipid-protein interactions and for the energetic of insertion of peptides and proteins in lipid aggregates. For biotechnological applications, the results are of interest for the optimization of the composition of lipid aggregates (bilayers and micelles) that can be used as carriers of hydrophobic ligands, including insoluble drugs.

Transparency document

The Transparency document associated with this article can be found in the online version.

Appendix A. Supplementary data

Supplementary data associated with this article can be found, in the online version, at https://doi.org/10.1016/j.chemphyslip.2019.03.005.

References

Afanasyeva, E.F., Syryamina, V.N., De Zotti, M., Formaggio, F., Toniolo, C., Dzuba, S.A., 2019. Peptide antibiotic trichogin in model membranes: self-association and capture of fatty acids. Biophys. Biochim. Acta-Biomembr. 1861, 524–531.

Anyarambhatla, G., Needham, D., 1999. Enhancement of the phase transition permeability of DPPC liposomes by incorporation of MPPC: a new temperature-sensitive liposome for use with mild hyperthermia. J. Liposome Res. 9 (491-), 506.

Arvidson, G., Brentel, I., Khan, A., Lindblom, G., Fontell, K., 1985. Phase equilibria in four lysophosphatidylcholine/water systems. Exceptional behaviour of 1-palmitoyl-glycero-phosphocholine. Eur. J. Biochem. 152, 753–759.

Bartucci, R., Pali, T., Marsh, D., 1993. Lipid chain motion in an interdigitated gel phase: conventional and saturation transfer ESR of spin-labeled lipids in dipalmitoylphosphatidylcholine-glycerol dispersions. Biochemistry 32, 274–281.

Bartucci, R., Guzzi, R., Marsh, D., Sportelli, L., 2003a. Intramembrane polarity by electron spin echo spectroscopy of labeled lipids. Biophys. J. 84, 1025–1030.

Bartucci, R., Belsito, S., Sportelli, L., 2003b. Spin-label electron spin resonance studies of micellar dispersions of Pegs-Pes polymer-lipids. Chem. Phys. Lip. 124, 11–122.

Bartucci, R., Guzzi, R., Sportelli, L., Marsh, D., 2009. Intramembrane water associated with TOAC spin-labeled alamethicin: electron spin-echo envelope modulation by D_2O. Biophys. J. 96, 997–1007.

Bartucci, R., Guzzi, R., Esmann, M., Marsh, D., 2014. Water penetration profile at the protein-lipid interface in Na,K-ATPase membranes. Biophys. J. 107, 1375–1382.

Bhamidipati, S.P., Hamilton, J.A., 1995. Interactions of Lyso 1-Palmitoylphosphatidylcholine with phospholipids: a ^{13}C and ^{31}P-NMR study. Biochemistry 34, 5666–5677.

Boggs, J.M., Rangaraj, G., Watts, A., 1989. Behavior of spin labels in a variety of interdigitated lipid bilayers. Biochim. Biophys. Acta 981, 243–253.

Bratt, P., McManus, H.J.D., Kevan, L., 1992. Electron spin echo modulation studies of doxylstearic acid spin probes in frozen dihexadecyl phosphate and dioctadecyldimethylammonium chloride vesicles: interaction of the spin probe with deuterated water and effects of cholesterol addition. J. Phys. Chem. 96, 5093–5096.

Carmieli, R., Papo, N., Zimmermann, H., Potapov, A., Shai, Y., Goldfarb, D., 2006. Utilizing ESEEM spectroscopy to locate the position of specific regions of membrane-active peptides within model membranes. Biophys. J. 90, 492–505.

Cieslak, J.A., Focia, P.J., Gross, A., 2010. Electron Spin-Echo Envelope Modulation (ESEEM) reveals water and phosphate interactions with the KcsA potassium channel. Biochemistry 49, 1486–1494.

De Simone, F., Guzzi, R., Sportelli, L., Marsh, D., Bartucci, R., 2007. Electron spin-echo studies of spin-labeled lipid membranes and free fatty acids interacting with human serum albumin. Biochim. Biophys. Acta 1768, 1541–1549.

Dikanov, S.A., Tsvetkov, Yu D., 1992. Electron Spin Echo Envelope Modulation (ESEEM) Spectroscopy. CRC Press, Boca Raton, FL.

Erilov, D.A., Bartucci, R., Guzzi, R., Shubin, A.A., Maryasov, A.G., Marsh, D., Dzuba, S.A., Sportelli, L., 2005. Water concentration profiles in membranes measured by ESEEM of spin-labeled lipids. J. Phys. Chem. B 109, 12003–12013.

Fuller, N., Rand, R., 2001. The influence of lysolipids on the spontaneous curvature and bending elasticity of phospholipid membranes. Biophys. J. 81, 243–254.

Guzzi, R., Rizzuti, B., Bartucci, R., 2012. Dynamics and binding affinity of spin-labeled stearic acids in beta-lactoglobulin: evidences from EPR spectroscopy and molecular dynamics simulation. J. Phys. Chem. B 116, 11608–11615.

Hiff, T., Kevan, L., 1989. Electron spin echo modulation studies of doxylstearic acid spin probes in frozen vesicles: interaction of the spin probe with D_2O and effects of cholesterol addition. J. Phys. Chem. 93, 1572–1575.

Kurad, D., Jeschke, G., Marsh, D., 2003. Lipid membrane polarity profiles by high-field EPR. Biophys. J. 85, 1025–1033.

Kurshev, V.V., Kevan, L., 1995. Electron spin echo modulation studies of doxylstearic acid spin probes in frozen vesicle solutions: interaction of the spin probe with 31P in the surfactant headgroups. J. Phys. Chem. 99, 10616–10620.

Lasic, D.D., 1993. Liposomes: From Physics to Applications. Elsevier, Amsterdam.

Lee, Y., Chan, S.I., 1977. Effect of lysolecithin on the structure and permeability of lecithin bilayer vesicles. Biochemistry 16, 1303–1309.

Lu, J.Z., Xu, Y.M., Chen, J.W., Huang, F., 1997. Effect of lysophosphatidylcholine on behaviour and structure of phosphatidylcholine liposomes. Sci. China Ser. C-Life Sci. 40, 622–629.

Lu, J.Z., Hao, Y.H., Chen, J.W., 2001. Effect of cholesterol on the formation of an interdigitated gel phase in lysophosphatidylcholine and phosphatidylcholine binary mixtures. J. Biochem. 129, 891–898.

Luquain, C., Sciorra, V., Morris, A., 2003. Lysophosphatidic acid signaling: how a small lipid does big things. Trends Biochem. Sci. 28, 377–383.

Marsh, D., 2001. Polarity and permeation profiles in lipid membranes. Proc. Natl. Acad. Sci. U.S.A. 98, 7777–7782.

Marsh, D., 2010. Spin-label EPR for determining polarity and proticity in biomolecular assemblies: transmembrane profiles. Appl. Magn. Reson. 37, 435–454.

Marsh, D., Watts, A., 1982. Spin-labeling and lipid-protein interactions in membranes. In: In: Jost, P.C.G., Hayes, O. (Eds.), Lipid-Protein Interactions, vol 2. Wiley-Interscience, New York, pp. 53–126.

McIntosh, T.J., Advani, S., Burton, R.E., Zhelev, D.V., Needham, D., Simon, S.A., 1995. Experimental tests for protrusion and undulation pressures in phospholipids bilayers.

Biochemistry 34, 8520–8532.
Mishima, K., Nakajima, M., Ogihara, T., 2004. Effects of lysophospholipids on membrane order of phosphatidylcholine. Colloids Surf. B-Biointerface 33, 185–189.
Needham, D., Anyarambhatla, G., Kong, G., Dewhirst, M.W., 2000. A new temperature-sensitive liposome for use with mild hyperthermia: characterization and testing in a human tumor xenograft model. Cancer Res. 60, 1197–1201.
Noethig-Laslo, V., Cevc, P., Arcon, D., Sentjurc, M., 2004. Comparison of CW-EPR and ESEEM technique for determination of water permeability profile in liposome membranes. Appl. Magn. Reson. 27, 303–309.
Ohata, H., Tanaka, K., Maeyama, N., Ikeuchi, T., Kamada, A., Yamanoto, M., Momose, K., 2001. Physiological and pharmacological role of lysophosphatidic acid as modulator in mechanotransduction. Jpn. J. Pharmacol. 87, 171–176.
Oranges, M., Guzzi, R., Marsh, D., Bartucci, R., 2018. Ether-linked lipids: spin-label EPR and spin echoes. Chem. Phys. Lipids 212, 130–137.
Pantusa, M., Sportelli, L., Bartucci, R., 2008. Phase behaviour of DPPC/Lyso-PPC mixtures by spin-label ESR and spectrophotometry. Spectroscopy 22, 153–163.
Salnikov, E.S., Erilov, D.A., Milov, A.D., Tsvetkov, Yu D., Peggion, C., Formaggio, F., Toniolo, C., Raap, J., Dzuba, S.A., 2006. Location and aggregation of the spin-labeled peptide Trichogin GA IV in a phospholipid membrane as revealed by pulsed EPR. Biophys. J. 91, 1532–1540.
Schweiger, A., Jeschke, G., 2001. Principles of Pulse Electron Paramagnetic Resonance. Oxford University Press, New York.
Subczynski, W.K., Wisniewska, A., Yin, J.J., Hyde, J.S., Kusumi, A., 1994. Hydrophobic barriers of lipid bilayer membranes formed by reduction of water penetration by alkyl chain unsaturation and cholesterol. Biochemistry 33, 7670–7681.
Szajdzinska-Pietek, E., Maldonado, R., Kevan, L., Jones, R.R.M., 1984. Electron spin resonance and electron spin echo modulation studies of N,N,N',N'-tetramethylbenzidine photoionizaton in anionic micelles: structural effects of tetramethylammonium cation counterion substitution for sodium cation in dodecyl sulphate micelles. J. Am. Chem. Soc. 106, 4675–4678.
Urban, L., Steinhoff, H.J., 2013. Hydrogen bonding to the nitroxide of protein bound spin labels. Mol. Phys. 111, 2873–2881.
van Echteld, C.J.A., De Kruijff, B., De Gier, J., 1980. Differential miscibility properties of various phosphatidylcholine/lysophosphatidylcholine mixtures. Biochim. Biophys. Acta 595, 71–81.
van Echteld, C.J.A., De Kruijff, B., Mandersloot, J.G., De Gier, J., 1981. Effects of lysophosphatidylcholines on phosphatidylcholine and phosphatidylcholine/cholesterol liposome systems as revealed by ^{31}P-NMR, electron microscopy and permeability studies. Biochim. Biophys. Acta 649, 211–220.
van Meer, G., Voelker, D.R., Feigenson, G.W., 2008. Membrane lipids: where they are and how they behave. Nat. Rev. Mol. Cell Biol. 9, 112–124.
Volkov, A., Dockter, C., Bund, T., Paulsen, H., Jeschke, G., 2009. Pulsed EPR determination for water accessibility to spin-labeled amino acid residues in LHCIIb. Biophys. J. 96, 1124–1141.
Zhelev, D.V., 1988. Material property characteristics for lipid bilayers containing lysolipid. Biophys. J. 75, 321–330.